DOI: 10.1002/chem.200902111

Synthesis and Optical Properties of Europium-Complex-Doped Inorganic/Organic Hybrid Materials Built from Oxo–Hydroxo Organotin Nano Building Blocks

Wei-Qiang Fan,[a, b] Jing Feng,[a, b] Shu-Yan Song,[a, b] Yong-Qian Lei,[a, b] Guo-Li Zheng,[a, b] and Hong-Jie Zhang*[a]

Abstract: Hybrid materials doped with novel europium complexes were synthesized using PMMA-*co*-Sn_{12}Clusters (copolymers from oxohydroxo-organotin dimethacrylate and methylmethacrylate) as the matrix material. Two types of hybrid materials were obtained: the physically doped product, PMMA-*co*-Sn_{12}Cluster/$Eu(TTA)_3$phen, and the grafted product, PMMA-*co*-Sn_{12}Cluster-*co*-[$EuAA(TTA)_2$phen] (TTA = 2-thenoyltrifluoroacetone, phen = phenanthroline and AA = acrylic acid). The hybrid materials exhibited characteristic luminescence of the Eu^{3+} ions, and also showed relative especial optical properties compared with samples just using PMMA as the matrix material. The PMMA-*co*-Sn_{12}Cluster matrix exhibited a high physical doping quantity of [$Eu(TTA)_3$phen], which can be attributed to the special structure of this kind of hybrid material. GPC (gel-permeation chromatography), TGA (thermogravimetric analysis), SEM, ^{1}H NMR, ICP (inductively coupled plasma), ^{119}Sn NMR, FTIR, and diffuse reflectance techniques were employed to characterize the structures and properties of these hybrid materials.

Keywords: europium · hybrid materials · luminescence · nanostructures · organotin

Introduction

Organic–inorganic hybrid materials built from nano building blocks as class II hybrid materials have attracted intensive attention, because of their multiple natures due to having organic and inorganic components in a single construction.[1] So far, varied functional hybrid materials have been obtained by choosing different inorganic clusters as nano building blocks, which have potential applications in catalysis,[2] optics,[3] and magnetic materials.[4] Organic polymers, which are mainly composed of flexible chains, have been commonly used as the matrix material for grafting inorganic clusters. Furthermore, the grafted inorganic clusters and flexible chains may make the hybrid polymer possess both a nanoscale microstructure, and also a soft skeleton with the capacity for modification. Since the oxo–hydroxo butyltin cluster $[(BuSn)_{12}O_{14}(OH)_6][OH]_2$ has been synthesized by mild methods,[5] it becomes a challenge to design inorganic/organic hybrid materials from butyltin-cluster nano building blocks.[6] Many efforts have been made to functionalize $[(BuSn)_{12}O_{14}(OH)_6]^{2+}$ with polymerizable anions and polyanionic spacers, which results in the formation of organic–inorganic hybrid materials.[7] Moreover, some of these hybrid materials can be easily dissolved in organic solvents, which is of interest for the formation of gels (or films). Based on the outstanding properties of such materials, it may be fascinating to attempt to form multifunctional hybrid materials based on the oxo–hydroxo butyltin cluster. However, to the best of our knowledge, there have been only a few reports on the further function of these hybrid materials, particularly in the optical area.[8] So, it may be most interesting to endow these hybrid materials with optical properties by doping (or grafting) functional complexes (such as rare earth complexes).

[a] Dr. W.-Q. Fan, Dr. J. Feng, Dr. S.-Y. Song, Dr. Y.-Q. Lei, Dr. G.-L. Zheng, Prof. H.-J. Zhang
Chinese Academy of Sciences
State Key Laboratory of Rare Earth Resource Utilization
Changchun Institute of Applied Chemistry
Changchun 130022 (P.R. China)
Fax: (+86) 431-85698041
E-mail: hongjie@ciac.jl.cn

[b] Dr. W.-Q. Fan, Dr. J. Feng, Dr. S.-Y. Song, Dr. Y.-Q. Lei, Dr. G.-L. Zheng
Graduate School of the Chinese Academy of Sciences
Beijing 100049 (P.R. China)

Supporting information for this article is available on the WWW under http://dx.doi.org/10.1002/chem.200902111.

Europium complexes are a useful class of luminophores, showing a strong red luminescence emission, attributed to the 4f–4f transitions of the Eu^{3+} ions.[9] The organic ligands in the europium complexes can not only transfer energy to Eu^{3+} ions by the "antenna effect", but also shield the metal ions from quenching interactions because of the strong bonding to the 4f metal center.[10] So, europium complexes exhibit relative stability and efficient emission under ultraviolet excitation, which is why europium complexes have been widely applied in organic–inorganic hybrid materials.[11] However, it is known that lanthanide complexes are usually hydrophobic, which makes doping, especially physical doping, difficult in inorganic matrices. In order to resolve this problem, on the one hand, many studies mainly focus on modifying the ligands with active groups to graft the lanthanide complexes onto the matrix, thus improving the doping capacity and dispersion of the lanthanide complexes in the matrix.[12] On the other hand, some studies use a matrix that is suitable for lanthanide complexes, such as an organic polymer. However, due to the anisotropism of the polymer matrix and lanthanide complexes, it is difficult to ensure that the lanthanide complexes are well dispersed in the polymer matrix when the physical doping method is chosen. Therefore, if the matrix possessed micro-spaces for holding lanthanide complexes, it would enhance physical doping and help to disperse the lanthanide complexes well in the matrix.

In this paper, we introduced europium complexes into the hybrid polymer-based oxo–hydroxo butyltin cluster to prepare novel hybrid materials. Two major strategies were designed for the synthesis of hybrid materials: 1) Synthesis of the polymer (PMMA-*co*-Sn_{12}Cluster) first, then doping with [Eu(TTA)$_3$phen] to obtain the PMMA-*co*-Sn_{12}Cluster/[Eu(TTA)$_3$phen] hybrid material; 2) synthesis of the PMMA-*co*-Sn_{12}Cluster-*co*-[EuAA(TTA)$_2$phen] hybrid material directly (PMMA = polymethylmethacrylate, TTA = 2-thenoyltrifluoroacetone, phen = phenanthroline and AA = acrylic acid). The structures of the hybrid materials were further characterized by GPC (gel-permeation chromatography), TGA (thermogravimetric analysis), and IR, ^{1}H NMR, and ^{119}Sn NMR spectroscopy. The photoluminescent properties of the two kinds of hybrid materials were also studied in detail.

Results and Discussion

The proposed mechanisms for the formation of PMMA-*co*-Sn_{12}Cluster/[Eu(TTA)$_3$phen] and PMMA-*co*-Sn_{12}Cluster-*co*-[EuAA(TTA)$_2$phen] are described in Scheme 1.

$[(BuSn)_{12}O_{14}(OH)_6][OH]_2$ was introduced into the hybrid materials through functionalization with two methacrylate (MA) groups. According to the IR spectra (Figure S1, Supporting Information), the $[(BuSn)_{12}O_{14}(OH)_6][MA]_2$ exhibited the typical ν(O–H) of Sn–OH at around 3650 cm^{-1}, and a new band at 1647 cm^{-1}, which can be attributed to the ν_{as}(C=C) of the MA. Four sharp bands (672, 623, 536, and 430 cm^{-1}) were due to the vibrations related to the Sn–O–Sn framework.[7a,13] The vibrations of Sn-O-Sn were not changed in the IR spectra of the hybrid materials (PMMA-*co*-Sn_{12}Cluster, PMMA-*co*- Sn_{12}Cluster/[Eu(TTA)$_3$phen], and PMMA-*co*-Sn_{12}Cluster-*co*-[EuAA(TTA)$_2$phen]), whereas the ν_{as}(C=C) disappeared. However, we cannot distinguish the bands of C=C (AA) from the [EuAA(TTA)$_2$phen] complex in the IR spectra, due to the presence of the TTA and phen ligands. Therefore, we further studied the polymerization of the AA group ([EuAA(TTA)$_2$phen]) through ^{1}H NMR spectroscopy. Referring to the ^{1}H NMR spectra, the proton absorption bands in [EuAA(TTA)$_2$phen] (δ = 6.35 ppm CH=CH_2, AA) and $\{(BuSn)_{12}O_{14}(OH)_6\}(MA)_2$ (δ = 5.87 and 5.21 ppm C(CH_3)=CH_2, MA) were no longer detected in the polymer products. Therefore, all the above results suggest that $[(BuSn)_{12}O_{14}(OH)_6][MA]_2$ and [EuAA(TTA)$_2$phen] were successfully grafted in the polymers.

^{119}Sn NMR spectroscopy (CD_2Cl_2) was performed to study whether the structure of the Sn_{12} cluster was retained in the hybrid materials. In Figure 1, ^{119}Sn NMR spectra of the hybrid materials (PMMA-*co*-Sn_{12}Cluster, PMMA-*co*-

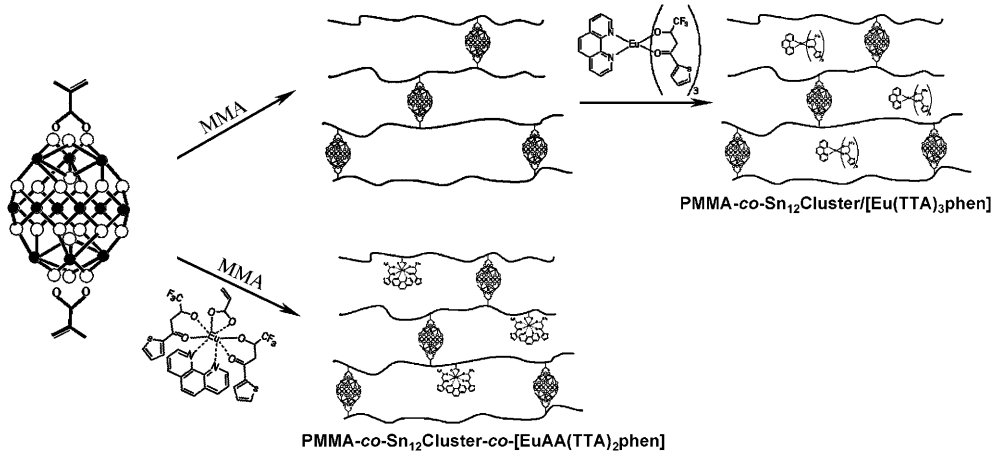

Scheme 1. The proposed mechanisms for the formation of PMMA-*co*-Sn_{12}Cluster/[Eu(TTA)$_3$phen] and PMMA-*co*-Sn_{12}Cluster-*co*-[EuAA(TTA)$_2$phen] hybrid materials.

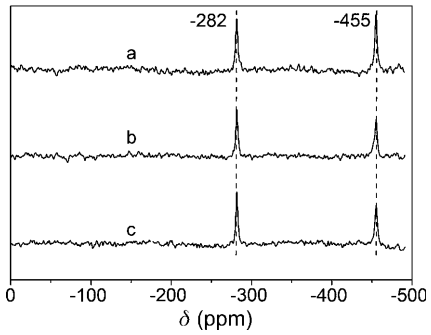

Figure 1. ^{119}Sn NMR spectra for a) PMMA-*co*-Sn_{12}Cluster, b) PMMA-*co*-Sn_{12}Cluster/[$Eu(TTA)_3$phen], and c) PMMA-*co*-Sn_{12}Cluster-*co*-[$EuAA(TTA)_2$phen].

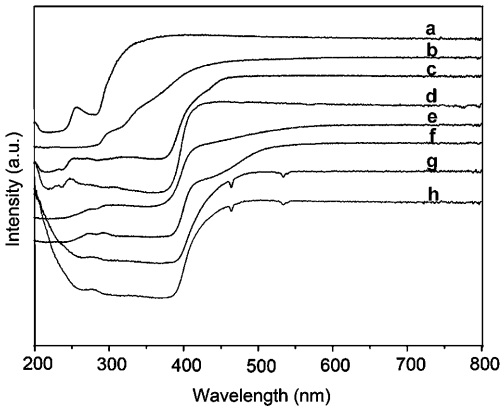

Figure 2. DR spectra of a) PMMA, b) PMMA-*co*-Sn_{12}Cluster, c) PMMA-*co*-[$EuAA(TTA)_2$phen], d) PMMA/[$Eu(TTA)_3$phen], e) PMMA-*co*-Sn_{12}Cluster-*co*-[$EuAA(TTA)_2$phen], f) PMMA-*co*-Sn_{12}Cluster/[$Eu(TTA)_3$phen], g) [$EuAA(TTA)_2$phen], and h) [$Eu(TTA)_3$phen].

Sn_{12}Cluster/[$Eu(TTA)_3$phen], and PMMA-*co*-Sn_{12}Cluster-*co*-[$EuAA(TTA)_2$phen]) all show the two characteristic resonances at −282 and −455 ppm, which correspond to the five- and six-coordinate tin atoms in the Sn_{12} cluster, respectively.[7a,8a,14] The two resonances are almost in a 1:1 ratio. Therefore, we assume that the structure of the Sn_{12} cluster in the hybrid materials was not broken, even after doping with europium complexes.

The molecular weight and the content of the Sn (Eu) in the hybrid materials were characterized by GPC, ICP (inductively coupled plasma), and TGA. The number average molecular weight (M_n) and polydispersity indexes (Table 1) of these samples are in the ranges of 8000–10000 and 1.2–1.4, respectively. The content of SnO_2 in the PMMA-*co*-Sn_{12}Cluster and PMMA-*co*-Sn_{12}Cluster-*co*-[$EuAA(TTA)_2$phen] are 26.4 and 28.5%, respectively, and the molar ratios of MMA and Sn_{12}Cluster in the products can be calculated from these results. The results indicate that the molar ratios of MMA and Sn_{12}Cluster in the products are a little lower than the feeding ratios. The Eu/Sn_{12}Cluster molar ratio, with the europium content determined by ICP in the PMMA-*co*-Sn_{12}Cluster-*co*-[$EuAA(TTA)_2$phen], is about 3.2% (the feeding ratio is 5%), and the europium (calculated as Eu_2O_3) content in the PMMA-*co*-[$EuAA(TTA)_2$phen] is 0.2%.

It is known that the Eu^{3+} ions in complexes can accept energy from the lowest triplet states of ligands with the help of resonant energy transfer, and then exhibit luminescence through f–f transitions. Therefore, the absorptions of the ligands and the matrix materials would significantly affect the luminescence of the Eu^{3+} ions. According to previous reports,[15] a diffuse reflection (DR)spectrum is a possible approach for studying the absorption of the materials. Here, DR spectra of our samples were investigated. In Figure 2, the DR spectra of PMMA-*co*-Sn_{12}Cluster-*co*-[$EuAA(TTA)_2$phen] and PMMA-*co*-Sn_{12}Cluster/[$Eu(TTA)_3$phen] exhibit composite spectra, which combine the spectra of europium complexes (250–400 nm) and the PMMA-*co*-Sn_{12}Cluster matrix (below 250 nm), indicating that the europium complexes have been doped successfully in these hybrid materials.[16] In addition, the DR spectra of PMMA-*co*-[$EuAA(TTA)_2$phen] and PMMA/[$Eu(TTA)_3$phen] show the same phenomena. However, the differences between the PMMA and MMA-*co*-Sn_{12}Cluster matrix are manifest at low wavelength: the absorption of PMMA-*co*-Sn_{12}Cluster extends to 200 nm, whereas PMMA just ends at 220 nm, perhaps due to the effect of the Sn_{12}clusters. It is worth noting that doping the Sn_{12}Clusters into hybrid materials extends the absorption spectra to lower wavelengths.

Based on the DR spectra, we further studied the photoluminescence (PL) spectra of the hybrid materials. PL spectroscopy is also an important method for investigating the chemical environment of Eu^{3+} ions. PL spectra of the europium complexes and hybrid materials doped with europium complexes are shown in Figure 3 (top). The excitation spectra of the hybrid materials have the same broad bands (250–400 nm) as the europium complexes, and these broad bands can be attributed to the absorption of the ligands in the europium complexes, which indicates energy transfer from the

Table 1. GPC, TGA, and ICP data of the products.

	SnO_2 (Eu_2O_3) content [wt%]	MMA/Sn_{12}Cluster[a]	M_n [g mol^{-1}]	M_w/M_n
PMMA-*co*-Sn_{12}Cluster	26.4	42:1	8781	1.31
PMMA-*co*-Sn_{12}Cluster-*co*-[$EuAA(TTA)_2$phen] (5%)	28.5[b]	37:1	8185	1.23
PMMA			9715	1.33
PMMA-*co*-[$EuAA(TTA)_2$phen] (5%)	0.2[c](Eu_2O_3)		8972	1.29

[a] Experimentally calculated MMA/Sn_{12}Cluster molar ratio in hybrid materials. [b] The Eu/Sn_{12}Cluster = 3.2% molar ratio was measured by ICP. [c] The Eu content was measured by ICP and calculated as Eu_2O_3.

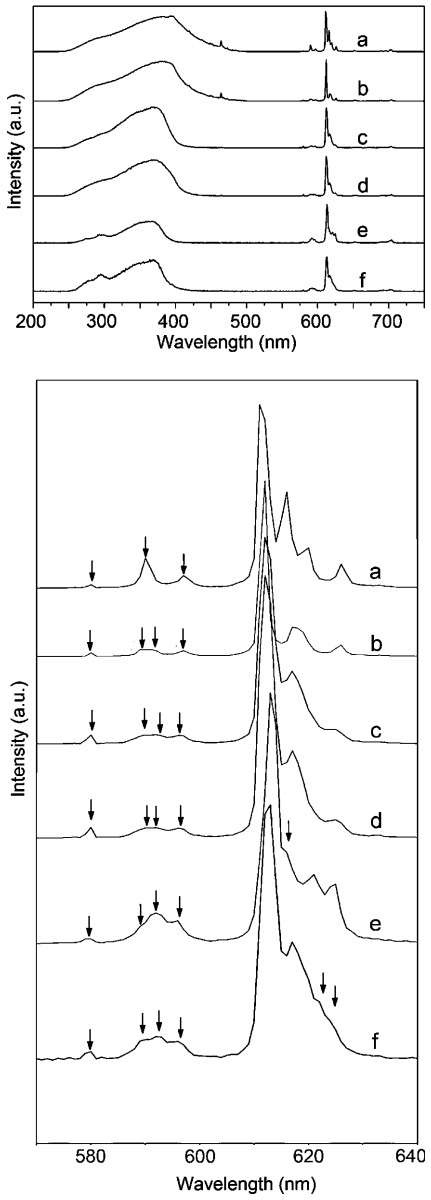

Figure 3. Top: PL spectra of a) [EuAA(TTA)$_2$phen], b) [Eu(TTA)$_3$phen], c) PMMA-*co*-[EuAA(TTA)$_2$phen], d) PMMA/[Eu(TTA)$_3$phen], e) PMMA-*co*-Sn$_{12}$Cluster-*co*-[EuAA(TTA)$_2$phen], and f) PMMA-*co*-Sn$_{12}$Cluster/Eu(TTA)$_3$phen]. All the excitation spectra were monitored at 612 nm. Bottom: Details of the $^5D_0 \rightarrow {}^7F_{0-2}$ transitions in the PL spectra.

ligands to the Eu^{3+} ions.[17] The results of the excitation spectra also show that the europium complexes keep their structure after being doped in the PMMA and PMMA-*co*-Sn$_{12}$Cluster matrix materials.

The emission spectra for europium complexes and europium-complex-doped hybrid materials, excited at around 370 nm, mainly exhibited luminescence: 580 ($^5D_0 \rightarrow {}^7F_0$), 590 ($^5D_0 \rightarrow {}^7F_1$), 612 ($^5D_0 \rightarrow {}^7F_2$), 650 ($^5D_0 \rightarrow {}^7F_3$), and 702 nm ($^5D_0 \rightarrow {}^7F_4$). The PL spectra are partially magnified in Figure 3 (bottom) in order to study the details of the $^5D_0 \rightarrow {}^7F_{0-2}$ transitions. We can see that: 1) the local ligand split the F_J levels into 2–3 ($^7F_1$) and 3–4 ($^7F_2$) Stark components; 2) the intensity of the $^5D_0 \rightarrow {}^7F_2$ transitions is distinctly higher than the $^5D_0 \rightarrow {}^7F_1$ transitions; 3) the $^5D_0 \rightarrow {}^7F_0$ transition exhibited just a single peak in all the samples. These results could confirm that the Eu^{3+} ions are at a low-symmetry site and are surrounded with a similar chemical environment.[18] The splitting of the F_2 levels in the PMMA-*co*-Sn$_{12}$Cluster matrix material into four Stark components, which are higher than that in the PMMA matrix material, might indicate that the local ligand field of the europium complexes was affected by the matrix materials built from oxo–hydroxo organotin nano building blocks.

The decay curves for europium complexes and europium-complex-doped hybrid materials are fitted by single exponential functions (Figure S2, Supporting Information), which further indicates that the Eu^{3+} ions are in the same average environment. The lifetimes of the $^5D_0 \rightarrow {}^7F_2$ transition of the samples are as follows (Table 2): [Eu(TTA)$_3$phen] (0.82 ms), [EuAA(TTA)$_2$phen] (0.83 ms), PMMA-*co*-Sn$_{12}$Cluster/[Eu(TTA)$_3$phen] (5%) (0.73 ms), PMMA-*co*-Sn$_{12}$Cluster-*co*-[EuAA(TTA)$_2$phen] (0.87 ms), PMMA/[Eu(TTA)$_3$phen] (5%) (0.56 ms), and PMMA-*co*-[EuAA(TTA)$_2$phen] (0.57 ms). Compared with the PMMA matrix, the lifetimes of Eu^{3+} ions in the PMMA-*co*-Sn$_{12}$Cluster matrix are relatively longer, which could indicate that the PMMA-*co*-Sn$_{12}$Cluster matrix may also play a role in protecting the Eu^{3+} ions from quenching.

It is known that the transition $^5D_0 \rightarrow {}^7F_1$ belongs to a magnetic dipolar transition that is insensitive to the surrounding environment of the Eu^{3+} ions, whereas $^5D_0 \rightarrow {}^7F_2$ is an electric dipolar transition, and the relative intensity ratio (R) of $^5D_0 \rightarrow {}^7F_2$ to $^5D_0 \rightarrow {}^7F_1$ can indicate how far the local environment of the Eu^{3+} ions is centrosymmetric.[19] In Table 2, we

Table 2. Photoluminescent data[a] of europium complexes and europium-complex-doped hybrid materials as solids.

	[Eu(TTA)$_3$phen]	[EuAA(TTA)$_2$phen]	PMMA-*co*-Sn$_{12}$Cluster/[Eu(TTA)$_3$phen] (5%)	PMMA-*co*-Sn$_{12}$Cluster-*co*-[EuAA(TTA)$_2$phen]	PMMA/[Eu(TTA)$_3$phen] (5%)	PMMA-*co*-[EuAA(TTA)$_2$phen]
R	24.1	6.0	8.5	7.8	22.7	19.7
τ [ms]	0.82	0.83	0.73	0.87	0.56	0.57
A_{rad}^{0-4}	596	430	544	421	708	697
A_{nrad}^{0-4}	625	775	826	728	1078	1057
η [%]	48.4	35.7	39.8	36.6	39.6	39.7
n_w	0.3	0.5	0.6	0.5	0.8	0.8

[a] The emission intensity of the $^5D_0 \rightarrow {}^7F_1$ transition (I_{01}) and the $^5D_0 \rightarrow {}^7F_2$ transition (I_{02}), the intensity ratios ($R = I_{02}/I_{01}$) between the $^5D_0 \rightarrow {}^7F_2$ and $^5D_0 \rightarrow {}^7F_1$ transitions, lifetimes (τ), radiative decay rates (A_{rad}^{0-4}), nonradiative decay rates (A_{nrad}^{0-4}), and the emission quantum efficiency (η) of the $^5D_0$ excited state of Eu^{3+} ions, were obtained at room temperature; water molecules coordinated to the metal ions (n_w).

calculated the *R* value for the europium complexes and europium-complex-doped hybrid materials. Compared with europium complexes, the *R* value of the hybrid materials changed, especially for the hybrid materials using the PMMA-*co*-Sn_{12}Cluster as matrix. Among all the *R* values, we are very interested in that of the PMMA-*co*-Sn_{12}Cluster/[Eu(TTA)$_3$phen], for the following two reasons: 1) the *R* value of the PMMA-*co*-Sn_{12}Cluster/[Eu(TTA)$_3$phen] (5%) has changed distinctly relative to [Eu(TTA)$_3$phen]; 2) compared with PMMA-*co*-Sn_{12}Cluster/[Eu(TTA)$_3$phen] (5%), the *R* value of the PMMA/[Eu(TTA)$_3$phen] (5%) hardly altered. According to a previous report,[8a] the introduction of Sn_{12}Clusters into the polymer materials may make the materials have high polarity, which may affect the centrosymmetric environment of the Eu^{3+} ions, and thus influence the *R* value.

Inspired by the observations above, we reason that the *R* value of the luminescence may be used to study the dispersing condition of Eu(TTA)$_3$phen in PMMA-*co*-Sn_{12}Cluster. As previously reported, the introduction of lanthanide complexes into the silicate matrix through sol–gel methods has been widely studied,[20] but the hard property of the silicate matrix results in a difficulty with extensively doping lanthanide complexes, especially through physical mixing (commonly less than 1% molar ratio); also, the excess europium complexes will induce the second lanthanide complex phase in the silicate matrix. Here, we synthesized a series of PMMA-*co*-Sn_{12}Cluster/*x*[Eu(TTA)$_3$phen] hybrid materials ($x=0.1$, 1, 2, 5, and 10%). In Figure 4, their excitation and emission spectra are almost consistent, except for the intensities. As calculated (Table 3), the *R* values of samples with different doping quantities of [Eu(TTA)$_3$phen] did not change on the whole, even up to 10%. It seems that a large quantity of [Eu(TTA)$_3$phen] doped in the PMMA-*co*-Sn_{12}Cluster matrix could be well dispersed and may not aggregate as the second phase in the matrix material, because the *R* values would change if the second phase of the [Eu(TTA)$_3$phen] was formed, due to the significant difference of *R* value between [Eu(TTA)$_3$phen]-doped hybrid materials and pure [Eu(TTA)$_3$phen]. The reason for the high capacity of doping europium complex could be attributed to the special structure of this kind of matrix material. As we know, the main structure of this matrix material is composed of soft chains (PMMA), which are bridged with nano building blocks (Sn_{12}clusters). This kind of structure will endow this matrix material with a relatively flexible framework and nanospace supported by the Sn_{12}clusters, which may be conducive to doping europium complexes. This is a fascinating property which may remedy this defect of the silicate matrix. Therefore, this kind of hybrid material built from Sn_{12}cluster nano building blocks may be an alternative matrix material for lanthanide complexes.

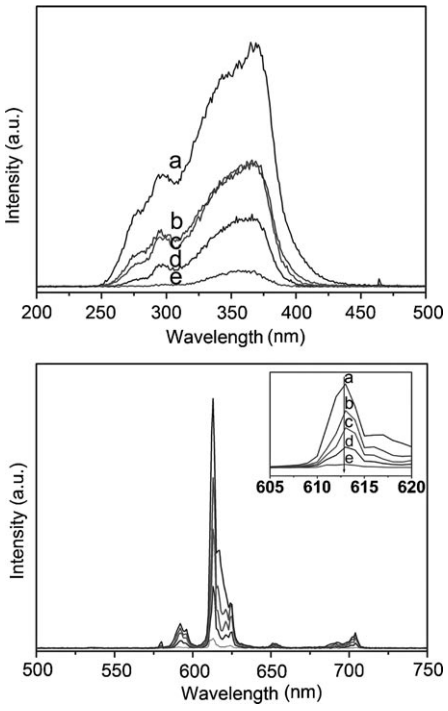

Figure 4. Excitation and emission spectra for PMMA-*co*-Sn_{12}Cluster/*x*[Eu(TTA)$_3$phen] hybrid materials: a) $x=10$, b) $x=5$, c) $x=2$, d) $x=1$, and e) $x=0.1$%.

Table 3. *R* values for a series of PMMA-*co*-Sn_{12}Cluster/Eu(TTA)$_3$phen hybrid materials (0.1, 1, 2, 5, and 10%).

	R[I($^5D_0\rightarrow{}^7F_2$)/I($^5D_0\rightarrow{}^7F_1$)]
PMMA-*co*-Sn_{12}Cluster/[Eu(TTA)$_3$phen] (0.1%)	9.2
PMMA-*co*-Sn_{12}Cluster/[Eu(TTA)$_3$phen] (1%)	8.2
PMMA-*co*-Sn_{12}Cluster/[Eu(TTA)$_3$phen] (2%)	7.7
PMMA-*co*-Sn_{12}Cluster/[Eu(TTA)$_3$phen] (5%)	8.5
PMMA-*co*-Sn_{12}Cluster/[Eu(TTA)$_3$phen] (10%)	9.7

According to the emission spectra and lifetimes of the $^5D_0$ emitting level, the emission quantum efficiency (η) of the $^5D_0$ level and the number of water molecules coordinated to the Eu^{3+} ions (n_w) can be calculated (Table 2). The lifetime, radiative (A_{rad}), and nonradiative (A_{nrad}) transition rates are related through Equation (1).[21]

$$\frac{1}{\tau}=A_{rad}+A_{nrad} \quad (1)$$

The radiative contribution for the $^5D_0\rightarrow{}^7F_5$ and $^5D_0\rightarrow{}^7F_6$ transitions should be neglected as they are very weak in the spectra. The magnetic dipole $^5D_0\rightarrow{}^7F_1$ transition, which is relatively insensitive to the chemical environments around the Eu^{3+} ion, can be considered as a reference for the whole spectrum. Then, A_{rad} could be obtained by Equation (2),[22] in which ν_{01} and ν_{0J} are the energy baricenters of the $^5D_0\rightarrow{}^7F_1$ and $^5D_0\rightarrow{}^7F_J$ transitions, respectively, I_{01} and I_{0J} are the integrated intensities of $^5D_0\rightarrow{}^7F_1$ and $^5D_0\rightarrow{}^7F_J$, respectively, and A_{01} is Einstein's coefficient of spontaneous emission between the $^5D_0$ and $^7F_1$ levels and could be considered to be equal to 50 s^{-1}.[23]

$$A_{\mathrm{rad}} = A_{01}\frac{v_{01}}{I_{01}}\sum_{J=0}^{4}\frac{I_{0J}}{v_{0J}} = \sum\nolimits_{J} A_{0J} \quad (2)$$

Assuming that only nonradiative and radiative processes are involved in the depopulation of the $^5D_0$ state of Eu^{3+}, η may be defined as in Equation (3).[9c]

$$\eta = \frac{A_{rad}}{A_{rad} + A_{nrad}} \quad (3)$$

Furthermore, the water molecules (n_w) coordinated to the metal ions in the hybrid materials can also be estimated through the A_{rad} data, as shown in Equations (4) and (5) (the units of A_{rad} should be ms^{-1} in this section).

$$A_{\mathrm{exp}} = \frac{1}{\tau} \quad (4)$$

$$n_w = 1.1 \times \left(A_{\mathrm{exp}} - A_{rad} - 0.31\right) \quad (5)$$

All the calculated results are shown in Table 2. Compared with [Eu(TTA)$_3$phen] ($\eta = 48.4\,\%$), the η value of the PMMA-*co*- Sn_{12}Cluster/[Eu(TTA)$_3$phen] and PMMA/[Eu(TTA)$_3$phen] lowered to around 39%, which is mainly attributed to the increase of A_{nrad}. We consider that the molecular high-energy vibration of the main flexible framework groups (PMMA) in hybrid materials might play a role in nonradiative transitions; this has also been reported in the literature.[24]

However, it is surprising that the η values of PMMA-*co*-Sn_{12}Cluster-*co*-[EuAA(TTA)$_2$phen] and PMMA-*co*-[EuAA(TTA)$_2$phen] are higher than that of [EuAA(TTA)$_2$phen]. Although the main flexible framework groups have an adverse effect on the η value, we should also consider that the [EuAA(TTA)$_2$phen] was grafted on the PMMA chains. This would fix the [EuAA(TTA)$_2$phen] on the skeleton, and then enable the [EuAA(TTA)$_2$phen] molecules to separate from each other in the hybrid materials, and also depress the molecular vibrations of the [EuAA(TTA)$_2$phen]. A combination of the above reasons would cause the enhancement of the η values of the grafted hybrid materials.

The η values in the PMMA and PMMA-*co*-Sn_{12}Cluster matrix materials are similar, so we think that the europium complexes doped in the PMMA-*co*-Sn_{12}Cluster matrix materials are mostly surrounded by PMMA chains, and the Sn_{12}Cluster plays the role of a bridge and does not react (or assemble) with the europium complexes. The relatively high η values (all around 39%) of the hybrid materials also partially result from the small number of water molecules coordinated to the Eu^{3+} ions, because the water molecules would strongly quench the luminescence of the Eu^{3+} ions. The calculated number of water molecules is no more than one molecule, which is advantageous for the luminescence efficiency.

On the other hand, the structures of these hybrid materials are mainly composed of soft chains; this will make these kinds of hybrid materials dissolve easily in organic solvents to form films (or gels), and will enhance the transparency of the films (or gels). So, we sequentially tried to prepare hybrid films using THF solutions of these hybrid materials (Figure 5). The hybrid films we obtained were transparent on the glass substrates, and exhibited strong red luminescence when irradiated with UV light. Furthermore, the SEM images showed a smooth surface and section at high magnification, which indicated that the films were formed with a homogeneous matrix. The facile dissolution in organic solvent and easy gellation under mild conditions provide these kinds of hybrid materials with shape controllability, which may lead to more widespread applications of hybrid materials doped with europium complexes in the optical field.

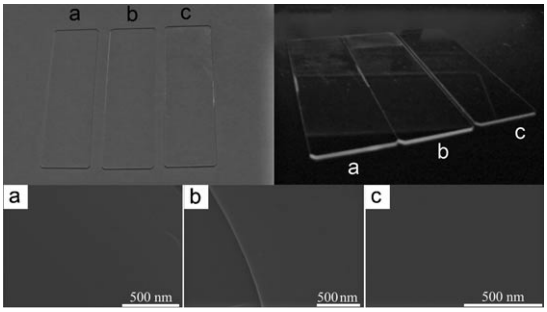

Figure 5. Photos of the transparent films on the glass substrates and under UV light irradiation. The lower part shows the SEM images of the films. a) PMMA-*co*-Sn_{12}Cluster-*co*-[EuAA(TTA)$_2$phen] film, b) PMMA-*co*-Sn_{12}Cluster/[Eu(TTA)$_3$phen] film, and c) PMMA-*co*-Sn_{12}Cluster film; scale bars = 500 nm.

Conclusions

Luminescent hybrid materials, based on physically doping (or covalently bonding) europium complexes into PMMA-*co*-Sn_{12}Cluster, have been prepared successfully. Due to the nanoscale space microstructure and soft skeleton, the PMMA-*co*-Sn_{12}Cluster matrix could be grafted easily with europium complexes, and also has a high capacity for physical doping of europium complexes. Compared with the single PMMA matrix, PMMA-*co*-Sn_{12}Cluster has more extensive absorption spectra in the low wavelength region in the DR spectra. It could also play a role in protecting the Eu^{3+} ions from quenching, which would maintain the lifetimes of the europium complexes. The emission quantum efficiency (η) of the $^5D_0$ level and the number of water molecules (n_w) coordinated to the Eu^{3+} ions were calculated from the luminescence data. The luminescent hybrid materials could be redissolved in organic solvent and repeatedly gelled, which endows the luminescent hybrid materials with shape controllability. The transparent films formed on the glass substrates are homogeneous and exhibit red luminescence under UV light. The novel character of these hybrid materials will provide access to investigate further the opti-

cal properties of other lanthanide complexes in these kinds of hybrid materials.

Experimental Section

Solid reagents were of analytical grade and used as received without further purification. Liquid reagents were used after desiccation.

Synthesis of polymer: PMMA-*co*-Sn_{12}Cluster: $[(BuSn)_{12}O_{14}(OH)_6][OH]_2$ ($[Sn_{12}Cluster][OH]_2$) was synthesized according to previous reports.[25] Then $[(BuSn)_{12}O_{14}(OH)_6][MA]_2$ and the polymer were prepared according to reference [7b]. A 10 wt% solution of $[(BuSn)_{12}O_{14}(OH)_6][MA]_2$ in THF was added to methylmethacrylate (MMA) (MMA:cluster = 30:1). The reaction mixture was heated at 70 °C for 60 h using 2,2′-azobis(isobutyronitrile) (AIBN; 5% molar ratio of the methacrylic group) as radical initiator. The entire procedure was performed under N_2. Finally, the polymer was obtained by precipitation of the product in diethyl ether. $[(BuSn)_{12}O_{14}(OH)_6][MA]_2$: ^{1}H NMR (400 MHz, $CDCl_3$, 25 °C, TMS): δ = 5.87, 5.21 (s, 4H; $(CH_3)C{=}CH_2$), 1.90 (s, 6H; $(CH_3)C{=}CH_2$), 1.16 (m, 24H; $CH_2CH_2CH_2CH_3$), 1.72, 1.57 (m, 24H; $CH_2CH_2CH_2CH_3$), 1.32 (m, 24H; $CH_2CH_2CH_2CH_3$), 0.94, 0.87 ppm (tt, J = 7.2 Hz, 36H; $CH_2CH_2CH_2CH_3$).

PMMA-*co*-Sn_{12}Cluster physically doped with the [Eu(TTA)$_3$phen] complex (PMMA-*co*-Sn_{12}Cluster/[Eu(TTA)$_3$phen]): The $[Eu(TTA)_3phen]$ complex was synthesized following the literature procedure.[26] The $[Eu(TTA)_3phen]$ complex was dissolved in tetrahydrofuran (THF), then added dropwise into a THF solution of PMMA-*co*-Sn_{12}Cluster, with Eu/Sn_{12}Cluster molar ratios equal to 0.1, 1, 2, 5, and 10% respectively. The solution was stirred for 30 min and then dried in air for two days.

Synthesis of PMMA-*co*-Sn_{12}Cluster-*co*-[EuAA(TTA)$_2$phen]: $[EuAA(TTA)_2phen]$ was prepared by the methods described in the literature.[27] The synthesis procedure for MMA-*co*-Sn_{12}Cluster-*co*-$[EuAA(TTA)_2phen]$ was also similar to that of PMMA-*co*-Sn_{12}Cluster, except that $[EuAA(TTA)_2phen]$ (Eu/Sn_{12}Cluster molar ratio = 5%) was added to the reaction mixture. $[EuAA(TTA)_2phen]$: ^{1}H NMR (400 MHz, $[D_6]$DMSO, 25 °C, TMS): δ = 9.11, 8.51, 8.00, 7.79 (8H; phen CH), 7.45, 7.22, 7.03 (6H; TTA CH), 6.35 ppm (3H; CH=CH_2); IR (KBr): 1581 and 1417 (COO), 1520 (phen C=C), 1600 (coordinated C=O), 416 cm^{-1} (Eu–O). PMMA-*co*-Sn_{12}Cluster-*co*-$[EuAA(TTA)_2phen]$: ^{1}H NMR (400 MHz, $CDCl_3$, 25 °C, TMS): δ = 3.66 ($COOCH_3$), 1.83 (CH_2), 1.75–1.19 ($CH_2CH_2CH_2CH_3$), 1.18 and 0.83 (CH_3 of the MMA), 0.95 ppm ($CH_2CH_2CH_2CH_3$).

Preparation of the films: The transparent films from PMMA-*co*-Sn_{12}Cluster, PMMA-*co*-Sn_{12}Cluster/$[Eu(TTA)_3phen]$, and PMMA-*co*-Sn_{12}Cluster-*co*-$[EuAA(TTA)_2phen]$ were easily prepared as follows: dissolution of the samples in THF, then immersion of the clean glass substrates into the solution, slow lifting of the glass substrates, and, finally, drying of the glass substrates in air.

PMMA, PMMA/[Eu(TTA)$_3$phen], and PMMA-*co*-[EuAA(TTA)$_2$phen]: These were synthesized using the same procedures as above but without $[(BuSn)_{12}O_{14}(OH)_6][MA]_2$. PMMA-*co*-$[EuAA(TTA)_2phen]$ and PMMA/$[Eu(TTA)_3phen]$ were in molar ratio: $[EuAA(TTA)_2phen]$/30MMA = 5%, and $[Eu(TTA)_3phen]$/30MMA = 5%.

Characterization: Field-emission scanning electron microscopy (FESEM) images were obtained with a XL30 ESEM FEG microscope. Room-temperature photoluminescence (PL) spectra were recorded on a Fluorolog-3 with a 450 W xenon lamp as the excitation source at room temperature. The decay curves for the $^5D_0 \rightarrow {}^7F_2$ (612 nm) emission of the samples were measured with a UV laser beam. FTIR spectra were measured within a 4000–400 cm^{-1} region on an American BIO-RAD Company model FTS135 infrared spectrophotometer using the KBr pellet technique. The diffuse reflectance (DR) measurements were recorded on a SHIMADZU UV-3600 spectrophotometer. ^{1}H NMR and ^{119}Sn NMR spectra were recorded on Bruker AV-400 spectrometer; ^{119}Sn NMR spectra (CD_2Cl_2) were obtained under proton decoupling and chemical shifts are relative to external tetramethyltin. TGA measurements were performed on a Perkin–Elmer Thermal Analysis Pyris Diamond TG/DTA. The samples were heated under air from 40 to 800 °C at a heat rate of 10 °C min^{-1}. The content of Eu^{3+} ions was obtained by inductively coupled plasma-atomic emission spectroscopy (ICP-AES-MS) with a TJA-POEMS spectrometer. The molecular weights and molecular weight distributions of the samples were determined in THF with a Gel Permeation Chromatography (GPC) instrument using WATERS-410GPC equipped with WATO44219 HT6E.

Acknowledgements

The authors are grateful for financial aid from the National Natural Science Foundation of China (grant nos. 20631040 and 20771099) and the MOST of China (grant nos. 2006CB601103 and 2006DFA42610).

[1] a) C. Sanchez, G. J. de A. A. Soler-Illia, F. Ribot, T. Lalot, C. R. Mayer, V. Cabuil, *Chem. Mater.* **2001**, *13*, 3061–3083; b) C. Sanchez, G. J. de A. A. Soler-Illia, F. Ribot, D. Grosso, *C. R. Acad. Sci. Ser. IIc C. R. Chim.* **2003**, *6*, 1131–1151; c) G. Kickelbick, U. Schubert, *Monatsh. Chem.* **2001**, *132*, 13–30.

[2] a) L. Zhang, H. C. L. Abbenhuis, Q. H. Yang, Y. M. Wang, P. C. M. M. Magusin, B. Mezari, R. A. Santen, C. Li, *Angew. Chem.* **2007**, *119*, 5091–5094; *Angew. Chem. Int. Ed.* **2007**, *46*, 5003–5006; b) A. Shimojima, R. Goto, N. Atsumi, K. Kuroda, *Chem. Eur. J.* **2008**, *14*, 8500–8506.

[3] a) H. L. Li, W. Qi, W. Li, H. Sun, W. F. Bu, L. X. Wu, *Adv. Mater.* **2005**, *17*, 2688–2692; b) W. Qi, H. L. Li, L. X. Wu, *Adv. Mater.* **2007**, *19*, 1983–1987.

[4] F. Palacio, P. Oliete, U. Schubert, I. Mijatovic, N. Hüsing, H. Peterlik, *J. Mater. Chem.* **2004**, *14*, 1873–1878.

[5] a) F. Banse, F. Ribot, P. Tolédano, J. Maquet, C. Sanchez, *Inorg. Chem.* **1995**, *34*, 6371–6379; b) C. Eychenne-Baron, F. Ribot, N. Steunou, C. Sanchez, *Organometallics* **2000**, *19*, 1940–1949.

[6] F. Ribot, C. Eychenne-Baron, C. Sanchez, *Phophorus Sulfur and Silicon* **1999**, *150–151*, 41–58.

[7] a) F. Ribot, F. Banse, F. Diter, C. Sanchez, *New J. Chem.* **1995**, *19*, 1145–1153; b) F. Ribot, F. Banse, C. Sanchez, M. Lahcini, B. Jousseaume, *J. Sol-Gel Sci. Technol.* **1997**, *8*, 529–533; c) L. Angiolini, D. Caretti, R. De Vito, F. T. Niesel, E. Salatelli, C. Carlini, F. Ribot, C. Sanchez, *J. Inorg. Organomet. Polym.* **1997**, *7*, 151–162.

[8] a) F. Ribot, A. Lafuma, C. Eychenne-Baron, C. Sanchez, *Adv. Mater.* **2002**, *14*, 1496–1499; b) C. Sanchez, B. Lebeau, F. Chaput, J. P. Boilot, *Adv. Mater.* **2003**, *15*, 1969–1994.

[9] a) X. M. Guo, L. S. Fu, H. J. Zhang, L. D. Carlos, C. Y. Peng, J. F. Guo, J. B. Yu, R. P. Deng, L. N. Sun, *New J. Chem.* **2005**, *29*, 1351–1358; b) S. Gago, J. A. Fernandes, J. P. Rainho, R. A. SáFerreira, M. Pillinger, A. A. Valente, T. M. Santos, L. D. Carlos, P. J. A. Ribeiro-Claro, I. S. Goncüalves, *Chem. Mater.* **2005**, *17*, 5077–5084; c) P. C. R. Soares-Santos, H. I. S. Nogueira, V. Felix, M. G. B. Drew, R. A. S. Ferreira, L. D. Carlos, T. Trindade, *Chem. Mater.* **2003**, *15*, 100–108.

[10] L. D. Carlos, R. A. S. Ferreira, V. de Zea Bermudez, S. J. L. Ribeiro, *Adv. Mater.* **2009**, *21*, 509–534.

[11] a) R. A. Sá Ferreira, L. D. Carlos, R. R. Gonçalves, S. J. L. Ribeiro, V. de Zea Bermudez, *Chem. Mater.* **2001**, *13*, 2991–2998; b) H. R. Li, P. Liu, Y. G. Wang, L. Zhang, J. B. Yu, H. J. Zhang, B. Y. Liu, U. Schubert, *J. Phys. Chem. C* **2009**, *113*, 3945–3949; c) L. H. Wang, W. Wang, W. G. Zhang, E. T. Kang, W. Huang, *Chem. Mater.* **2000**, *12*, 2212–2218; d) Y. Okamoto, Y. Ueba, N. F. Dzhanibekov, E. Banks, *Macromolecules* **1981**, *14*, 17–22; e) A. C. Franville, D. Zambon, R. Mahiou, Y. Troin, *Chem. Mater.* **2000**, *12*, 428–435.

[12] a) P. Liu, H. R. Li, Y. G. Wang, B. Y. Liu, W. J. Zhang, Y. J. Wang, W. D. Yan, H. J. Zhang, U. Schubert, *J. Mater. Chem.* **2008**, *18*, 735–737; b) F. Y. Liu, L. S. Fu, J. Wang, Z. Liu, H. R. Li, H. J. Zhang, *Thin Solid Films* **2002**, *419*, 178–182; c) P. Lenaerts, K. Driesen, R. VanDeun, K. Binnemans, *Chem. Mater.* **2005**, *17*, 2148–2154.

[13] H. Reuter, A. Sebald, *Z. Naturforsch. B* **1993**, *48*, 195–198.
[14] F. Ribot, D. Veautier, S. Guillaudeu, T. Lalot, *J. Sol-Gel Sci. Technol.* **2004**, *32*, 37–41.
[15] a) J. Feng, J. B. Yu, S. Y. Song, L. N. Sun, W. Q. Fan, X. M. Guo, S. Dang, H. J. Zhang, *Dalton Trans.* **2009**, 2406–2414; b) J. Feng, S. Y. Song, Y. Xing, H. J. Zhang, Z. F. Li, L. N. Sun, X. M. Guo, W. Q. Fan, *J. Solid State Chem.* **2009**, *182*, 435–441.
[16] L. N. Sun, H. J. Zhang, L. S. Fu, F. Y. Liu, Q. G. Meng, C. Y. Peng, J. B. Yu, *Adv. Funct. Mater.* **2005**, *15*, 1041–1048.
[17] C. Y. Peng, H. J. Zhang, J. B. Yu, Q. G. Meng, L. S. Fu, H. R. Li, L. N. Sun, X. M. Guo, *J. Phys. Chem. B* **2005**, *109*, 15278–15287.
[18] M. Fernandes, V. de Zea Bermudez, R. A. SáFerreira, L. D. Carlos, A. Charas, J. Morgado, M. M. Silva, M. J. Smith, *Chem. Mater.* **2007**, *19*, 3892–3901.
[19] a) Y. S. Liu, W. Q. Luo, R. F. Li, G. K. Liu, M. R. Antonio, X. Y. Chen, *J. Phys. Chem. C* **2008**, *112*, 686–694; b) P. P. Yang, Z. W. Quan, C. X. Li, H. Z. Lian, S. S. Huang, J. Lin, *Microporous Mesoporous Mater.* **2008**, *116*, 524–531; c) H. X. Mai, Y. W. Zhang, L. D. Sun, C. H. Yan, *Chem. Mater.* **2007**, *19*, 4514–4522; d) E. Guillet, D. Imbert, R. Scopelliti, J. C. G. Bünzli, *Chem. Mater.* **2004**, *16*, 4063–4070; e) F. Renaud, C. Piguet, G. Bernardinelli, J. C. G. Bünzli, G. Hopfgartner, *Chem. Eur. J.* **1997**, *3*, 1660–1667.
[20] a) S. Dang, L. N. Sun, H. J. Zhang, X. M. Guo, Z. F. Li, J. Feng, H. D. Guo, Z. Y. Guo, *J. Phys. Chem. C* **2008**, *112*, 13240–13247; b) L. N. Sun, H. J. Zhang, Q. G. Meng, F. Y. Liu, L. S. Fu, C. Y. Peng, J. B. Yu, G. L. Zheng, S. B. Wang, *J. Phys. Chem. B* **2005**, *109*, 6174–6182.
[21] H. R. Li, H. F. Shao, Y. G. Wang, D. H. Qin, B. Y. Liu, W. J. Zhang, W. D. Yan, *Chem. Commun.* **2008**, 5209–5211.
[22] E. E. S. Teotonio, J. G. P. Espínola, H. F. Brito, O. L. Malta, S. F. Oliveria, D. L. A. de Foria, C. M. S. Izumi, *Polyhedron* **2002**, *21*, 1837–1844.
[23] a) M. F. Hazenkamp, G. Blasse, *Chem. Mater.* **1990**, *2*, 105–110; b) M. H. V. Werts, R. T. F. Jukes, J. W. Verhoeven, *Phys. Chem. Chem. Phys.* **2002**, *4*, 1542–1548.
[24] X. M. Guo, H. D. Guo, L. S. Fu, R. P. Deng, W. Chen, J. Feng, S. Dang, H. J. Zhang, *J. Phys. Chem. C* **2009**, *113*, 2603–2610.
[25] C. Eychenne-Baron, F. Ribot, C. Sanchez, *J. Organomet. Chem.* **1998**, *567*, 137–142.
[26] L. R. Melby, N. J. Rose, E. Abramson, J. C. Caris, *J. Am. Chem. Soc.* **1964**, *86*, 5117–5125.
[27] a) L. Liu, Y. L. Lu, H. Lei, W. Zhang, C. Yang, Y. D. Liu, L. Q. Zhang, R. G. Jin, *Adv. Funct. Mater.* **2005**, *15*, 309–314; b) C. I. Lee, J. S. Lim, S. H. Kim, D. H. Suh, *Polymer* **2006**, *47*, 5253–5258.

Received: July 29, 2009
Published online: December 22, 2009

